

Essential contribution of a chemokine, CCL3, and its receptor, CCR1, to hepatocellular carcinoma progression

メタデータ	言語: eng 出版者: 公開日: 2017-10-05 キーワード (Ja): キーワード (En): 作成者: メールアドレス: 所属:
URL	http://hdl.handle.net/2297/6666

Running Title: CCR1 and CCL3 in hepatocellular carcinoma

ESSENTIAL CONTRIBUTION OF A CHEMOKINE, CCL3, AND ITS RECEPTOR, CCR1, TO HEPATOCELLULAR CARCINOMA PROGRESSION.

Xiaoqin Yang¹, Peirong Lu¹, Chifumi Fujii^{1,2}, Yasunari Nakamoto³, Ji-Liang Gao⁴, Shuichi Kaneko³, Philip M. Murphy⁴, and Naofumi Mukaida^{1,2*}

¹*Division of Molecular Bioregulation, Cancer Research Institute, Kanazawa University, Kanazawa, Japan*

²*Center for the Development of Molecular Target Drugs, Cancer Research Institute, Kanazawa University, Kanazawa, Japan*

³*Department of Gastroenterology, Graduate School of Medicine, Kanazawa University, Kanazawa, Japan*

⁴*Laboratory of Molecular Immunology, National Institute of Allergy and Infectious Diseases, National Institutes of Health, Bethesda, USA.*

*Correspondence to: Division of Molecular Bioregulation, Cancer Research Institute, Kanazawa University, 13-1 Takara-machi, Kanazawa 920-0934, Japan. Fax: 81-76-234-4520. E-mail: naofumim@kenroku.kanazawa-u.ac.jp

Key Words: *angiogenesis; chemokine; carcinogenesis; Kupffer cell; matrix metalloproteinase*

Abbreviations: bFGF, basic fibroblast growth factor; DEN, *N*-nitrosodiethylamine; HBs, hepatitis B virus surface antigen; HBV, human hepatitis B virus; HCC, hepatocellular carcinoma; HCV, human hepatitis C virus; HGF, hepatocytes growth factor; IMVD, intratumoral microvessel density; MMP, matrix metalloproteinase; RT-PCR, reverse transcription-polymerase chain reaction; TIMP, tissue inhibitor of matrix metalloproteinase; VEGF, vascular endothelial growth factor; WT, wild-type.

Grant sponsor: Ministry of Education, Culture, Sports, Science and Technology of the Japanese Government.

ABSTRACT

We previously observed that a chemokine, macrophage inflammatory protein-1 α /CCL3, and its receptor, CCR1, were aberrantly expressed in human hepatocellular carcinoma (HCC) tissues. Here, we show that CCL3 and CCR1 are also expressed in two different models of this cancer; *N*-nitrosodiethylamine (DEN)-induced HCC and HCC induced by hepatitis B virus surface (HBs) antigen-primed splenocyte transfer to myelo-ablated syngeneic HBs antigen transgenic mice. At 10 months after *N*-nitrosodiethylamine treatment, foci numbers and sizes were remarkably reduced in CCR1- and CCL3-deficient mice, compared with wild-type mice, although tumor incidence were marginally but significantly higher in CCR1- and CCL3-deficient mice than WT mice. Of note is that tumor angiogenesis was also markedly diminished in CCL3- and CCR1-deficient mice, with a concomitant reduction in the number of intratumoral Kupffer cells, a rich source of growth factors and matrix metalloproteinases (MMPs). Among growth factors and MMPs that we examined, only MMP9 and MMP13 gene expression was augmented progressively in liver of WT mice after DEN treatment. Moreover, MMP9 but not MMP13 gene expression was attenuated in CCR1- and CCL3-deficient mice, compared with wild-type mice. Furthermore, MMP9 was expressed mainly by mononuclear cells but not hepatoma cells, and MMP9-expressing cell numbers were decreased in CCR1- or CCL3-deficient mice, compared with wild-type mice. These observations suggest the contribution of the CCR1-CCL3 axis to HCC progression.

INTRODUCTION

Chemokines are a large family of chemoattractant cytokines for leukocytes^{1,2} and their receptors belong to a family of specific G protein-coupled seven-transmembrane domain receptors.³ A wide variety of tumor cells can produce various chemokines either constitutively or in response to various stimuli.⁴ Then, chemokines can recruit various types of leukocytes including monocytes/macrophages, lymphocytes, and dendritic cells, thereby modulating host responses to tumors. Moreover, several chemokines can control angiogenesis, a process essential for tumor growth, either directly or as a consequence of leukocyte infiltration and/or the induction of growth factor production.⁵ Furthermore, some chemokines can guide the growth and the motility of tumor cells,⁶ thereby affecting the processes of tumor progression.

Hepatocellular carcinoma (HCC) is endemic in Asia, Africa, and southern Europe, and ranks as the eighth most common cause of death among total human cancers. Most cases of HCC arise from chronic infection with human hepatitis B virus (HBV) or human hepatitis C virus (HCV).⁷ Although several lines of evidence suggest the potential involvement of the chemokine, interleukin-8/CXCL8 in the development of HCC,⁸⁻¹⁰ other chemokines and their receptors may also play a role. In this regard, among various chemokine receptors including CCR1, 2, 3, 4, and 5, CXCR1, 2, 3, and 4, we observed previously that CCR1 was the only one expressed constitutively in all the 6 human hepatoma cell lines that we examined.¹¹ Moreover, CCR1 and its ligand CCL3 were also expressed abundantly by tumor cells and to a lesser degree, endothelial cells in human HCC tissue.¹¹ These observations suggest that the CCL3-CCR1 axis can exert its effects on tumor cells as well as endothelial cells in an autocrine or paracrine manner.

Chronic HBV or HCV infection can cause continuous and recurrent cycles of hepatocyte necrosis and regeneration, resulting in accumulation of mutations.¹² Etiological studies have demonstrated that cigarette smoking increases the risk of HCC significantly among patients with chronic HBV infection because it contains *N*-nitrosamines, a potent class of hepatocarcinogen.^{13,14} Because *N*-nitrosodiethylamine (DEN), a specific *N*-nitrosamine, can cause HCC with a high frequency in rodents when administered to

suckling animals,^{15,16} the DEN-induced hepatocarcinogenesis model has been used to clarify the molecular mechanisms of hepatocarcinogenesis even though most cases of HCC arise from chronic infection of HBV or HCV.

Hence, in order to test the roles of CCL3 and CCR1 in hepatocarcinogenesis, we treated both wild-type mice and mice deficient in either *CCL3* or *CCR1* gene with DEN. Here, we provided the first definitive evidence on the contribution of the CCL3-CCR1 axis to HCC progression in an animal model.

MATERIAL AND METHODS

Reagents DEN was purchased from Sigma-Aldrich (St. Louis, MO). Rat anti-mouse F4/80 (clone: A3-1) and anti-CD34 (MEC 14.7) monoclonal antibodies were obtained from Serotec Ltd (Oxford, United Kingdom). Rabbit anti-mouse CCR1 antibodies were prepared¹⁷ and kindly provided by Dr. Kouji Matsushima (University of Tokyo). Goat anti-mouse CCL3 and goat anti-mouse matrix metalloproteinase (MMP) 9 antibodies were obtained from R&D Systems, Inc. (Minneapolis, MN).

Mice Specific pathogen-free C57BL/6 mice were purchased from Charles River Japan Co. (Yokohama, Japan) and designated as wild-type (WT) mice. CCL3-deficient mice¹⁸ were obtained from Jackson Laboratories (Bar Harbor, ME) and CCR1-deficient mice were generated as described previously.¹⁹ These deficient mice have been backcrossed to C57BL/6 mice for at least eight generations and were kept under specific pathogen-free conditions. The preparation of HBsAg transgenic mice were described previously.²⁰ These mice contain the entire HBV envelope containing region (subtype ayw) under the constitutive transcriptional control of the mouse albumin promoter and express the HBV small, middle, and large envelope proteins in their hepatocytes.²⁰ All animal experiments were performed in compliance with the Guideline for the Care and Use of Laboratory Animals on the Takara-machi Campus of Kanazawa University.

DEN-induced hepatocarcinogenesis model Three-week-old weanling male mice were given a single intraperitoneal injection of DEN dissolved in physiologic saline solution at a dose of 10 µg/g of body weight.²¹ Mice were killed 10 months after injection for the evaluation of HCC development. When mice died before this time interval, the liver was removed to enumerate the numbers of tumors on the liver surface larger than 1 mm, and to be fixed in 10% neutral-formalin buffer for histological analysis. In another series of experiments, mice were killed at the indicated time intervals after DEN treatment for histological analysis and extraction of total RNA.

Hepatocarcinogenesis model in HBs antigen transgenic mice Hepatocarcinogenesis was induced in HBs antigen transgenic mice by replacing bone marrow cells and splenocytes derived from syngeneic non-transgenic mice immunized with HBs antigen, as previously described.²² In this model, until 15 months after the splenocyte transfer, mice exhibited multiple HCC foci surrounded by non-tumor areas with hepatocytes with an atypical nuclear configuration.

Histological analysis Paraffin-embedded sections were cut at 5 μm and stained with hematoxylin and eosin solution. The numbers and sizes of the neoplastic foci were determined by an examiner without any prior knowledge about the experimental procedures, according to the method of Pierce²³ with some modifications. The foci number per cm^2 and the percentage of the areas occupied with tumor foci were determined by using NIH Image analysis software ver 1.62 (National Institutes of Health, Bethesda, MD).

Immunohistochemical analysis Rabbit anti-mouse CCR1 (5 $\mu\text{g}/\text{ml}$), goat anti-mouse CCL3 (10 $\mu\text{g}/\text{ml}$) or goat anti-mouse MMP9 antibodies (5 $\mu\text{g}/\text{ml}$) were used as the primary antibodies. The sections were further incubated with biotinylated goat anti-rabbit or rabbit anti-goat immunoglobulins as the secondary antibodies. The immune complexes were detected by using Vectastain Elite ABC kit and DAB Substrate Kit (Vector Laboratories, Burlingame, CA) according to the manufacturer's instructions. The slides were then counterstained with hematoxylin. The numbers of MMP9-expressing cells were counted on five randomly chosen fields from tumor and non-tumor areas in each animal at 400-fold magnification by an examiner without any prior knowledge of the experimental procedures.

Cell proliferation assay Human hepatoma-derived cell lines, HuH7 and HepG2 cells, were maintained in Dulbecco's modified essential medium (DMEM; Sigma chemical Co., St. Louis, MO) supplemented with 10% heat-inactivated fetal bovine serum (Atlanta Biological, Norcross, GA) in a humidified incubator at 37°C in 5% CO_2 . HuH7 and HepG2

cells were seeded into each well of a 96-multi-well plate at a cell density of 1×10^4 and 5×10^3 respectively, in the presence of recombinant human CCL3 (R&D Systems) at different concentrations. Forty-eight hours later, the cell viability was determined using WST-1 reagent (an MTT analog from Roche Diagnostics Corporation, Boehringer Mannheim) according to the manufacturer's instructions.

Enumeration of F4/80-positive cells Paraffin-embedded sections were deparaffinized in xylene and rehydrated through graded concentrations of ethanol. After serial treatment with 1% (w/v) hydrogen peroxide in methanol, the sections were incubated overnight at 4°C with rat anti-mouse F4/80 (1 µg/ml) to detect macrophages/Kupffer cells. Tissue sections were then incubated with biotin-conjugated anti-rat immunoglobulin antibody and treated with a Catalyzed Signal Amplification Kit (DAKO) according to the manufacturer's instructions. The numbers of F4/80-positive cells were counted on five randomly chosen fields in tumor as well as non-tumor areas in each animal at 200-fold magnification by an examiner without any prior knowledge of the experimental procedures. The area of each field is calculated to be 0.785 mm² and the numbers of F4/80-positive cells per mm² were calculated on both tumor and non-tumor areas.

CD34 immunohistochemical staining and intratumoral microvessel density (IMVD) determination After deparaffinization of the sections, the slides were treated with 1% (v/v) hydrogen peroxide in PBS for 10 min and trypsin for 20 min at 37°C. Thereafter, the sections were incubated overnight at 4°C with 5 µg/ml of rat anti-mouse CD34 monoclonal antibody, to determine IMVD.²⁴ Tissue sections were further incubated sequentially with biotin-conjugated anti-rat immunoglobulin antibody and ABC kit according to the manufacturer's instructions. The slides were then reacted with a Vectastain DAB Substrate Kit and counterstained with hematoxylin. CD34-positive areas in the tumor tissues were defined as the intratumoral vascular areas. Fields of abundant neovascularization (hot spots) were found by scanning the sections at low magnification ($\times 40$ or $\times 100$), and then the microvessel numbers as well as the pixel numbers of

CD34-positive areas were determined on five randomly chosen fields in hot spots of each animal at 200-fold magnification with the aid of Adobe Photoshop software Ver 7.0. IMVD was defined as the average numbers per one field at 200-fold magnification and the percentage area of blood vessels.

Semi-quantitative reverse transcription (RT)-polymerase chain reaction (PCR) Total RNA was extracted from a part of liver with RNazol B according to the manufacturer's instructions. After the RNA preparations were further treated with ribonuclease-free deoxyribonuclease (DNase) I (Life Technologies Inc., Gaithersburg, MD) to remove residual genomic DNA, cDNA was synthesized as described previously.¹¹ Serially two-fold diluted cDNA was amplified for β -actin using specific sets of primers (Table I) as described previously.¹¹ Thereafter, equal amounts of cDNA products were amplified for cytokines, matrix metalloproteinases (MMP), and tissue inhibitors of MMP (TIMP) using specific sets of primers based on the reported sequences (Table I), with the indicated cycle numbers of 94°C for 30 second, 55°C for 1 minute, and 72°C for 1 minute. The amplified PCR products were fractionated on a 1.5 % agarose gel and visualized by ethidium bromide staining. The intensities of the bands were measured with the aid of NIH Image Analysis software, and the ratios to β -actin were determined.

Statistical analysis Tumor incidence was analyzed by using χ^2 test for contingency table. All other data were analyzed statistically using one-way ANOVA followed by the Fisher's protected least significance difference test or Mann-Whitney's *U* test. $p < 0.05$ was considered as statistically significant.

RESULTS

CCL3 and CCR1 expression was enhanced progressively in two mouse models of HCC development We previously observed the constitutive expression of both CCL3 and its receptor, CCR1, in human HCC tissues.¹¹ Hence, in order to investigate the role of the CCL3-CCR1 axis in the HCC development, we first examined whether CCL3 and CCR1 proteins were expressed in mouse HCC arising in HBs antigen transgenic mice. We failed to detect any CCL3 and CCR1 protein expression in control mouse liver (Fig. 1*a-i, vi*). At 15 months after the HBs antigen-immunized splenocyte transfer, the liver possessed tumor areas surrounded by non-tumor areas as described previously.²² In non-tumor portions, a small number of hepatocytes were immunostained with anti-CCR1 (Fig. 1*a-ii*) or anti-CCL3 antibodies (Fig. 1*a-vii*). In contrast, tumor cells, some small bile duct cells, and endothelial cells were strongly stained with anti-CCR1 or CCL3 antibodies (Fig. 1*a-iii, iv, viii, and ix*). We next examined the expression patterns of CCL3 and CCR1 in mouse HCC induced by a chemical carcinogen, DEN. *CCL3* mRNA expression was faintly detected in liver from untreated WT mice, and enhanced progressively, thereafter. In contrast, *CCR1* gene expression was first detected 4 months after the treatment and was augmented progressively, thereafter (Fig. 1*b*). CCL3 protein was detected immunohistochemically occasionally on vascular endothelial cells in untreated mouse liver with no CCR1 expression (data not shown). Later than 2 months after DEN treatment, CCL3 protein was detected additionally in hepatocytes (Fig. 1*c-vi, vii*). At 10 months, CCL3 was evident in tumor cells (Fig. 1*c-viii*) and endothelial cells and some infiltrating mononuclear cells (Fig. 1*c-ix*). Concomitantly, CCR1 protein was expressed in tumor cells, vascular endothelial cells, and some infiltrating mononuclear cells (Fig. 1*c-iii, iv*). Thus, CCR1 and CCL3 were aberrantly expressed in liver in both hepatocarcinogenesis models.

Effects of CCL3 on human hepatoma cell lines Because CCR1 was expressed by hepatoma cells in both mouse and human,¹¹ we next evaluated the effects of CCL3 on human hepatoma cell lines. CCL3 inhibited the proliferation of human hepatoma cell lines

marginally but significantly at concentrations higher than 100 ng/ml (Fig. 2a, b). Because hepatoma cells could produce CCL3 abundantly only in response to interleukin 1 and other pro-inflammatory cytokines but not constitutively,¹¹ CCL3 may have some autocrine and/or paracrine effects on hepatoma cells.

Important roles of the CCR1-CCL3 axis to DEN-induced hepatocarcinogenesis In order to evaluate the contribution of CCR1 or CCL3 to DEN-induced hepatocarcinogenesis, we administered DEN to WT, CCR1-deficient, and CCL3-deficient mice. At 10 months after DEN treatment, there was a marginal but significant differences in terms of HCC incidence between CCR1-, and CCL3-deficient mice, compared with WT mice (5/13 cases, WT mice; 7/10, CCL3-deficient mice; 12/13, CCR1-deficient mice; $p < 0.05$). On the contrary, among tumor-bearing mice, the ratios of liver weights to body weights were significantly reduced in CCR1- and CCL3-deficient mice, compared with WT mice (Fig. 3a). Moreover, among tumor-bearing mice, the foci number per cm^2 and the proportion of tissues occupied with tumor were significantly decreased in CCL3- and to a lesser degree, CCR1-deficient mice, compared with WT mice (Fig. 3b, c). Since CCL3 can bind both CCR1 and CCR5,^{1,2} the compensatory effect of CCR5 in CCR1-deficient mice may account for a lesser reduction in tumor numbers and sizes in CCR1- than CCL3-deficient mice. Nevertheless, these results suggest the important roles of the CCR1-CCL3 axis in DEN-induced hepatocarcinogenesis.

Reduced intratumoral neovascularization and Kupffer cell accumulation in DEN-treated CCR1- and CCL3-deficient mice Reduced tumor foci number in CCR1- or CCL3-deficient mice may suggest that neovascularization, a prerequisite for hepatoma progression, was impaired in the absence of CCR1 or CCL3. Supporting this notion, both the microvessel numbers and the proportion of vascular areas in tumor areas were significantly reduced in CCL3- and CCR1-deficient mice, compared with wild-type mice (Fig. 4a, b). Because CCR1 is expressed by various types of cells including macrophages and Kupffer cells, a cellular source of various types of growth factors, we next determined macrophage and Kupffer cell numbers in HCC foci in WT and gene-deficient mice. In

tumor areas, the numbers of F4/80-positive cells were remarkably depressed in both CCR1- and CCL3-deficient mice, compared with WT mice, although the numbers of F4/80-positive cells in non-tumor areas were only modestly reduced in CCL3- but not CCR1-deficient mice, compared with WT mice (Fig. 4c). Because F4/80 antigen is expressed by both Kupffer cells and blood-derived macrophages, a more specific marker for blood-derived macrophages, ER-MP20,²⁵ was used. However, we detected few, if any, ER-MP20-positive cells in this model (data not shown). These observations would indicate that the CCL3-CCR1 axis has a crucial role also in the accumulation of F4/80-positive Kupffer cells into tumor areas in this DEN-induced hepatocarcinogenesis.

Reduced MMP-9 expression in liver from DEN-treated CCR1- and CCL3-deficient mice

We next investigated the gene expression of potent angiogenic factors, vascular endothelial growth factor (VEGF), basic fibroblast growth factor (bFGF), and hepatocyte growth factor (HGF) by RT-PCR. The gene expression of these angiogenic factors did not change significantly in WT mice, at any time after DEN injection that we examined (Fig. 5a). Similar results were obtained for the expression of VEGF receptors, *Flk-1* and *Flt-1* (Fig. 5a). Moreover, there were no significant differences in terms of the expression of these factors and receptors between WT and CCL3- or CCR1-deficient mice (data not shown). Because the balance between MMP and TIMP has crucial roles in the degradation of extracellular matrix proteins and subsequent angiogenesis, we next determined the gene expression of MMP and TIMP. Among MMP and TIMP that we examined, *MMP9* and *MMP13* gene expression was augmented progressively in WT mouse liver after DEN treatment (Fig. 5b). Moreover, *MMP9* but not *MMP13* gene expression was remarkably reduced in CCL3- and CCR1-deficient mice, compared with WT mice (Fig. 5c). We further observed that MMP9 proteins were detected in mononuclear cells accumulated inside hepatoma tissues arising in both DEN-treated mice (Fig. 5d) and HBs antigen transgenic mice (data not shown). We cannot exclude completely the possibility that HCC cells express MMP9 below the detection limit of the present immunohistochemical analysis. Nevertheless, it is likely that a major source of MMP9 was mononuclear cells in these

models. Moreover, the numbers of MMP9-positive cells in tumor sites were significantly decreased in CCR1- or CCL3-deficient mice, compared with WT mice (Fig. 5*d, e*).

DISCUSSION

DEN, a potent chemical hepatocarcinogen, acts as an initiator to cause a G-C to A-T transition mutation through the methylation of guanine.²⁶ As a result, when suckling rodents were given DEN, HCC developed with a high frequency with minimal inflammatory changes.^{15,16} Myelo-depleted HBs transgenic mice developed HCC until 15 months after the transfer of splenocytes obtained from syngeneic non-transgenic mice that had been primed with HBs antigen.²² This hepatocarcinogenesis occurred in the presence of chronic hepatitis, as observed in human HCC associated with chronic HBV or HCV infection.⁷ Here, we have provided definitive evidence that CCL3 and CCR1 were expressed aberrantly in tumor cells in these two distinctive murine hepatocarcinogenesis models. Thus, together with our previous observations on human HCC tissues,¹¹ these results suggest the generality of the aberrant expression of CCR1 and CCL3 in HCC tissues.

In order to define the roles of the CCL3-CCR1 axis in hepatocarcinogenesis, we administered DEN to CCR1- and CCL3-deficient mice as well as WT mice. Interestingly, both CCL3 and CCR1 affected both HCC initiation and tumor progression, but in opposite ways. Whereas HCC occurred more frequently in both CCL3- and CCR1-deficient mice compared to WT controls, tumor burden (foci number and the proportion of the organ occupied by tumor) was dramatically reduced in the former mice. The precise mechanisms underlying these effects are not yet clear, however our data point to several intriguing possibilities. With regard to disease initiation, we found that recombinant CCL3 stimulation of hepatoma cell lines is able to retard cell growth *in vitro* in a concentration-dependent manner. *In vivo* this could potentially translate into a growth disadvantage for newly transformed hepatocarcinoma cells, thereby facilitating surveillance and eradication of these cells by immune-mediated mechanisms. The net result would be decreased incidence of HCC in WT mice as compared with CCL3- or CCR1-deficient mice.

Maeda and colleagues demonstrated that NF- κ B activation in hepatocytes could be protective for DEN-induced hepatocarcinogenesis, while NF- κ B activation in intrahepatic hematopoietic cells could promote it.²⁷ Evidence is accumulating to indicate that CCR1-mediated signal could activate NF- κ B in several types of cells.^{28,29} Moreover, we

observed that CCR1 was expressed by hepatocytes and intrahepatic mononuclear cells. Thus, the net effects of the CCR1-CCL3 system may be a balance between its capacities to activate NF- κ B in these two distinct types of cells. In the initial step when mononuclear cells were scarce in liver, the CCR1-CCL3 system may activate NF- κ B, mainly in hepatocytes, which may account for a lower HCC incidence in WT mice than CCR1- or CCL3-deficient mice. Our data indicate that CCL3 and CCR1 are important for mononuclear cell accumulation in tumor, consistent with their known chemotactic effects in vitro and that some of these cells express a major angiogenic factor, MMP9 whose gene expression can be induced by NF- κ B activation.³⁰ Because angiogenesis is presumed to be crucially required for HCC progression,³¹ these combined effects could be a major factor restricting the size of tumors in CCL3- and CCR1-deficient mice.

Although several lines of evidence implied VEGF as an essential mediator regulating hypervascularity in HCC,^{32,33} we failed to detect any changes in VEGF and its receptor gene expression during the whole course of DEN-induced hepatocarcinogenesis. Moreover, we did not see any differences in VEGF and its receptor gene expression in liver between WT and either CCR1- or CCL3-deficient mice. Thus, it is unlikely that VEGF was a main mediator controlling angiogenesis in this model.

Evidence is accumulating to indicate that the balance between MMP and their inhibitors, TIMP, has crucial roles in tumor progression by inducing tumor angiogenesis and altering the extracellular environment more suitable for tumor cell establishment and growth.³⁴ Moreover, several cDNA microarray analyses on human HCC have revealed that the expression of some MMPs were enhanced in HCC tissues, compared with non-tumor portion.^{35,36} These observations prompted us to examine MMP and TIMP gene expression by RT-PCR analysis. Among MMPs and TIMPs that we examined, only *MMP9* and *MMP13* gene expression were augmented progressively after DEN treatment, and *MMP9* but not *MMP13* gene expression was significantly attenuated in liver of DEN-treated CCR1- and CCL3-deficient mice, compared with WT mice. Crucial involvement of MMP9 in angiogenesis has been substantiated by the observations on MMP9-deficient mice.³⁷ Moreover, MMP9-positive cells appeared even in pre-malignant lesion in the absence of

neovascularization (our unpublished data) and MMP9-positive cell numbers in tumor areas were significantly reduced in CCR1- or CCL3-deficient mice, compared with WT mice. Thus, it is likely that the reduction in MMP9 expression can account for attenuated tumor angiogenesis in CCR1- and CCL3-deficient mice.

Several lines of evidence indicate that bone marrow-derived progenitors can direct neovascularization.^{38,39} Moreover, CCL3 exhibits a potent mobilizing activity for hematopoietic stem cells⁴⁰ by predominantly interacting with CCR1.⁴¹ Furthermore, MMP9 was required for hematopoietic stem cell mobilization from bone marrow to other organs including liver.^{42,43} We also detected the presence of c-kit-positive stem cells co-expressing CCR1 in the tumor foci of DEN-treated but not untreated WT mice (our unpublished data). Thus, it is tempting to speculate that HCC-derived CCL3 induced hematopoietic stem cell mobilization into liver, in collaboration with MMP9 and that hematopoietic stem cells can induce tumor angiogenesis, in concert with MMP9.

Several gene loci, which have been identified as the loci determining the sensitivity of hepatocytes to DEN, are localized on mouse chromosomes 1, 2, 7, 8, and 12.⁴⁴ The present results suggest that both CCR1 and CCL3 have profound effects on the progression of DEN-induced hepatocarcinogenesis. Because *CCR1* and *CCL3* genes are localized on mouse chromosomes 9 and 11, respectively, these genes must be hitherto unidentified genes that determine the sensitivity to DEN-induced hepatocarcinogenesis. Moreover, given that both CCL3 and CCR1 were expressed by HCC cells, it is likely that the CCL3-CCR1 axis has some direct effects on HCC cells and can eventually regulate HCC progression induced by DEN treatment. Furthermore, aberrant expression of CCL3 and CCR1 was also observed in human HCC tissues¹¹ as well as in our murine hepatocarcinoma models in DEN-treated mice and HBs transgenic mice. Thus, CCL3 and CCR1 may be involved in the progression of HCC in general. If so, detailed molecular analysis on DEN-treated CCL3- or CCR1-deficient mice will shed a novel light on the molecular pathogenesis of HCC.

ACKNOWLEDGEMENTS

We thank Drs. T. Kondo, Y. Ishida (Department of Legal Medicine, Wakayama Medical University), T. Irimura, K. Denda-Nagai (Graduate School of Pharmaceutical Sciences, University of Tokyo), and M. Naito (Graduate School of Medical and Dental Sciences, Niigata University) for their invaluable advice on the immunostaining.

REFERENCES

1. Baggiolini M. Chemokines and leukocyte traffic. *Nature* 1998;392:565-8.
2. Luster AD. Chemokines-chemotactic cytokines that mediate inflammation. *N Engl J Med* 1998;338:436-45.
3. Premack BA, Schall TJ. Chemokine receptors: gateways to inflammation and infection. *Nat Med* 1996;2:1174-8.
4. Brault MS, Kurt RA. Chemokines and antitumor immunity: walking the tightrope. *Int Rev Immunol* 2003;22:199-28.
5. Bernardini G, Ribatti D, Spinetti G, Morbidelli L, Ziche M, Santoni A, Capogrossi MC, Napolitano M. Analysis of the role of chemokines in angiogenesis. *J Immunol Methods* 2003;273:83-101.
6. Homey B, Muller A, Zlotnik A. Chemokines: agents for the immunotherapy of cancer? *Nat Rev Immunol* 2002;2:175-84.
7. Sell S. Mouse models to study the interaction of risk factors for human liver cancer. *Cancer Res* 2003;63:7553-62.
8. Mahe Y, Mukaida N, Kuno K, Akiyama M, Ikeda N, Matsushima K, Murakami S. Hepatitis B virus X protein transactivates human interleukin-8 gene through acting on nuclear factor κ B and CCAAT/enhancer-binding protein-like cis-elements. *J Biol Chem* 1991;266:13759-63.
9. Polyak SJ, Khabar KS, Paschal DM, Ezelle HJ, Duverlie G, Barber GN, Levy DE, Mukaida N, Gretch DR. Hepatitis C virus nonstructural 5A protein induces interleukin-8, leading to partial inhibition of the interferon-induced antiviral response. *J Virol* 2001;75:6095-106.
10. Iguchi A, Kitajima I, Yamakuchi M, Ueno S, Aikou T, Kubo T, Matsushima K, Mukaida N, Maruyama I. PEA3 and AP-1 are required for constitutive IL-8 gene expression in hepatoma cells. *Biochem Biophys Res Commun* 2000;279:166-71.
11. Lu P, Nakamoto Y, Nemoto-Sasaki Y, Fujii C, Wang H, Hashii M, Ohmoto Y, Kaneko S, Kobayashi K, Mukaida N. Potential interaction between CCR1 and its ligand, CCL3,

- induced by endogenously produced interleukin-1 in human hepatomas. *Am J Pathol* 2003;162:1249-58.
12. Geller SA. Hepatitis B and hepatitis C. *Clin Liver Dis* 2002;6:317-34.
 13. Chen CJ, Chen DS. Interaction of hepatitis B virus, chemical carcinogen, and genetic susceptibility: multistage hepatocarcinogenesis with multifactorial etiology. *Hepatology* 2002;36:1046-9.
 14. Berger MR, Schmahl D, Edler L. Implications of the carcinogenic hazard of low doses of three hepatocarcinogenic N-nitrosamines. *Jpn J Cancer Res* 1990;81:598-606.
 15. Yang X, Bhaumik M, Bhattacharyya R, Gong S, Rogler CE, Stanley P. New evidence for an extra-hepatic role of N-acetylglucosaminyltransferase III in the progression of diethylnitrosamine-induced liver tumors in mice. *Cancer Res* 2000;60:3313-9.
 16. Lee YS, Kim WH, Yu ES, Kim MR, Lee MJ, Jang JJ. Time course of cell cycle-related protein expression in diethylnitrosamine-initiated rat liver. *J Hepatol*. 1998;29:464-9.
 17. Tokuda A, Itakura M, Onai N, Kimura H, Kuriyama T, Matsushima K. Pivotal role of CCR1-positive leukocytes in bleomycin-induced lung fibrosis in mice. *J Immunol* 2000;164:2745-51.
 18. Cook DN, Beck MA, Coffman TM, Kirby SL, Sheridan JF, Pragnell IB, Smithies O. Requirement of MIP-1 α for an inflammatory response to viral infection. *Science* 1995;269:1583-5.
 19. Gao JL, Wynn TA, Chang Y, Lee EJ, Broxmeyer HE, Cooper S, Tiffany HL, Westphal H, Kwon-Chung J, Murphy PM. Impaired host defense, hematopoiesis, granulomatous inflammation and type 1-type 2 cytokine balance in mice lacking CC chemokine receptor 1. *J Exp Med* 1997;185:1959-68.
 20. Chisari FV, Filippi P, McLachlan A, Milich DR, Riggs M, Lee S, Palmiter RD, Pinkert CA, Brinster RL. Expression of hepatitis B virus large envelope polypeptide inhibits hepatitis B surface antigen secretion in transgenic mice. *J Virol* 1986;60:880-7.
 21. Nakano H, Hatayama I, Satoh K, Suzuki S, Sato K, Tsuchida S. c-Jun expression in single cells and preneoplastic foci induced by diethylnitrosamine in B6C3F1 mice:

- comparison with the expression of pi-class glutathione S-transferase. *Carcinogenesis* 1994;15:1853-7.
22. Nakamoto Y, Guidotti LG, Kuhlen CV, Fowler P, Chisari FV. Immune pathogenesis of hepatocellular carcinoma. *J Exp Med* 1998;188:341-50.
 23. Pierce RH, Vail ME, Ralph L, Campbell JS, Fausto N. Bcl-2 expression inhibits liver carcinogenesis and delays the development of proliferating foci. *Am J Pathol* 2002;160:1555-60.
 24. Martin L, Green B, Renshaw C, Lowe D, Rudland P, Leinster SJ, Winstanley J. Examining the technique of angiogenesis assessment in invasive breast cancer. *Brit J Cancer* 1997;76:1046-54.
 25. Leenen PJ, Melis M, Slieker WA, Van Ewijk W. Murine macrophage precursor characterization. II. Monoclonal antibodies against macrophage precursor antigens. *Eur J Immunol* 1990;20:27-34.
 26. Nakatsuru Y, Matsukuma S, Nemoto N, Sugano H, Sekiguchi M, Ishikawa T. O₆-methylguanine-DNA methyltransferase protects against nitrosamine-induced hepatocarcinogenesis. *Proc Natl Acad Sci. USA* 1993;90:6468-72.
 27. Maeda S, Kamata H, Luo JL, Leffert H, Karin M. IKK β couples hepatocytes death to cytokine-driven compensatory proliferation that promotes chemical hepatocarcinogenesis. *Cell* 2005;121:977-90.
 28. Omoike OI, Teague RM, Benedict SH, Chan MA. MIP-1 α induces binding of nuclear factors to the κ B DNA element in human B cells. *Mol Cell Biol Res Commun* 2000;4:15-9.
 29. Ness TL, Carpenter KJ, Ewing JL, Gerard CJ, Hogaboam CM, Kunkel SL. CCR1 and CC chemokine ligand 5 interactions exacerbate innate immune response during sepsis. *J Immunol* 2004;173:6938-48.
 30. Xie Z, Singh M, Singh K. Differential regulation of matrix metalloproteinase-2 and -9 expression and activity in adult rat cardiac fibroblasts in response to interleukin-1 β . *J Biol Chem* 2004;279:39513-9.
 31. Okuda K. Early recognition of hepatocellular carcinoma. *Hepatology* 1986;6:729-38.

32. Mise M, Arii S, Higashituji H, Furutani M, Niwano M, Harada T, Ishigami S, Toda Y, Nakayama H, Fukumoto M, Fujita J, Imamura M. Clinical significance of vascular endothelial growth factor and basic fibroblast growth factor gene expression in liver tumor. *Hepatology* 1996;23:455-64.
33. Miura H, Miyazaki T, Kuroda M, Oka, T, Machinami R, Kodama T, Shibuya M, Makuuchi M, Yazaki Y, Ohnishi S. Increased expression of vascular endothelial growth factor in human hepatocellular carcinoma. *J Hepatol* 1997;27:854-61.
34. John A, Tuszynski G. The role of matrix metalloproteinases in tumor angiogenesis and tumor metastasis. *Pathol Oncol Res* 2001;7:14-23.
35. Okabe H, Satoh S, Kato T, Kitahara O, Yanagawa R, Yamaoka Y, Tsunoda T, Furukawa Y, Nakamura Y. Genome-wide analysis of gene expression in human hepatocellular carcinomas using cDNA microarray: identification of genes involved in viral carcinogenesis and tumor progression. *Cancer Res* 2001;61:2129-37.
36. Chen X, Cheung ST, So S, Fan ST, Barry C, Higgins J, Lai K-M, Ji J, Dudoit S, Ng IOL, van deRijn M, Botstein D, Brown PO. Gene expression patterns in human liver cancers. *Mol Biol Cell* 2002;13:1929-39.
37. Vu TH, Shipley JM, Bergers G, Berger JE, Helms JA, Hanahan D, Shapiro SD, Senior RM, Werb Z. MMP-9/gelatinase B is a key regulator of growth plate angiogenesis and apoptosis of hypertrophic chondrocytes. *Cell* 1998;93:411-22.
38. Bagley RG, Walter-Yohrling J, Cao X, Weber W, Simons B, Cook BP, Chartrand SD, Wang C, Madden SL, Teicher BA. Endothelial precursor cells as a model of tumor endothelium: characterization and comparison with mature endothelial cells. *Cancer Res* 2003;63:5866-73.
39. Takakura N, Watanabe T, Suenobu S, Yamada Y, Noda T, Ito Y, Satake M, Suda T. A role for hematopoietic stem cells in promoting angiogenesis. *Cell* 2000;102:199-209.
40. Lord BI, Woolford LB, Wood LM, Czaplewski LG, McCourt M, Hunter MG, Edwards RM. Mobilization of early hematopoietic progenitor cells with BB-10010: A genetically engineered variant of human macrophage inflammatory protein-1 α . *Blood* 1995;85:3412-5.

41. Broxmeyer HE, Cooper S, Hangoc G, Gao JL, Murphy PM. Dominant myelopoietic effector functions mediated by chemokine receptor CCR1. *J Exp Med* 1999;189:1987-92.
42. Kollet O, Shivtiel S, Chen YQ, Suriawinata J, Thung SN, Dabeva MD, Kahn J, Spiegel A, Dar A, Samira S, Goichberg P, Kalinkovich A, Arenzana-Seisdedos F, Nagler A, Hardan I, Revel M, Shafritz DA, Lapidot T. HGF, SDF-1, and MMP-9 are involved in stress-induced human CD34⁺ stem cell recruitment to the liver. *J Clin Invest* 2003;112:160-9.
43. Heissig B, Hattori K, Dias S, Friedrich M, Ferris B, Hackett NR, Crystal RG, Besmer P, Lyden D, Moore MA, Werb Z, Rafii S. Recruitment of stem and progenitor cells from the bone marrow niche requires MMP-9 mediated release of kit-ligand. *Cell* 2002;109:625-37.
44. Gariboldi M, Manenti G, Canzian F, Falvella FS, Pierotti MA, Della Porta G, Binelli G, Dragani TA. Chromosome mapping of murine susceptibility loci to liver carcinogenesis. *Cancer Res* 1993;53:209-11.

Table I - The sequences of the primers and the conditions used for RT-PCR analysis

	Sense primer	Antisense primer	Cycles	Product (bp)
<i>β-actin</i>	TGTGATGGTGGGAATGGGTCAAG	TTTGATGTCACGCACGATTCC	25	514
<i>CCR1</i>	TTTAAGGCCAGTGGGAGTT	TGGTATAGCCACATGCCTTT	32	475
<i>CCL3</i>	ATCATGAAGGTCTCCACCAC	TCTCAGGCATTCAGTCCAG	32	284
<i>VEGF</i>	CTGCTGTACCTCCACCATGCCAAGT	CTGCAAGTACGTTTCGTTAACTCA	35	509
<i>bFGF</i>	ACACGTCAAACACTACAACCTCA	TCAGCTCTTAGCAGACATTGG	35	295
<i>HGF</i>	GCTTGGCATCCACGATGTTC	CCCTCACATGGTCTTGATCC	35	387
<i>Flt-1</i>	TTAGGGGGTTCTCCATACCC	TATCTTCATGGAGGCCTTGG	35	531
<i>Flk-1</i>	CAGCTTCCAAGTGGCTAAGG	CATAATGGAATTTGGGGTCG	35	620
<i>MMP2</i>	GAGTTGGCAGTGCAATACCT	GCCGTCCTTCTCAAAGTTGT	35	666
<i>MMP9</i>	AGTTTGGTGTGCGGAGCAC	TACATGAGCGCTTCCGGCAC	35	754
<i>MMP13</i>	CTGGTCTTCTGGCACACGCT	GCAGCGCTCAGTCTTTCAC	35	610
<i>TIMP-1</i>	CTGGCATCCTCTTGTTGCTA	AGGGATCTCCAGGTGCACAA	35	583
<i>TIMP-2</i>	AGACGTAGTGATCAGGGCCA	GTACCACGCGCAAGAACCAT	35	490

LEGENDS TO FIGURES

Figure 1 - Aberrant expression of CCR1 and CCL3 in hepatocarcinogenesis

(a) Immunohistochemical detection of CCR1 and CCL3 in HBs antigen transgenic mice. Immunohistochemical analysis using anti-CCR1 (*i-iv*), anti-CCL3 antibodies (*vi-ix*), or species-matched control antibodies (*v, x*) was performed on control liver (*i, vi*) and, non-tumor (*ii, vii*) and tumor portions (*iii, iv, v, viii, ix* and *x*) in liver in HBs antigen transgenic mice at 15 months after splenocyte transfer as described in Material and Methods. Representative results from three individual animals are shown here. The arrows in *iii* and *viii* indicate positively-stained bile duct and endothelial cells. *iv* and *ix* indicate positively-stained HCC cells. Original magnification, $\times 100$ (*i* and *vi*), $\times 200$ (*ii, iii, vii, viii*), $\times 400$ (*iv, v, ix, x*). Scale bars, 50 μm .

(b) *CCR1* and *CCL3* mRNA expression in liver after DEN treatment. RT-PCR was performed on total RNA extracted from WT mice liver at 0, 2, 4, 6, and 10 months after DEN treatment, as described in Material and Methods. Representative results from five individual experiments are shown here.

(c) Immunohistochemical analysis of CCR1 and CCL3 protein in WT mice liver after DEN treatment. Liver tissues were obtained from WT mice at 2 (*i, vi*), 6 (*ii, vii*), and 10 months after DEN treatment (*iii, iv, v, viii, ix, and x*). Immunohistochemical analysis was performed using anti-CCR1 (*i-iv*), anti-CCL3 antibodies (*vi-ix*), or species-matched control antibodies (*v, x*) as described in Material and Methods. Arrows in *iii* and *viii* indicate positively-stained HCC cells while an arrow in *iv* indicates positively-stained endothelial cells. The arrows and the inset (scale bar, 10 μm) in *ix* indicate infiltrating lymphocytes. Representative results from 3 animals from each time point are shown here. Original magnification, $\times 100$ (*i, ii*), $\times 200$ (*vi, vii*), $\times 400$ (*iii* to *v* and *viii* to *x*). Scale bars, 50 μm .

Figure 2 - The effects of CCL3 on hepatoma cell lines.

Either HuH7 (*a*) or HepG2 (*b*) cells were incubated in the presence of the indicated

concentrations of CCL3, and cell proliferation rates were assessed as described in Material and Methods. Similar experiments were repeated three times and representative results are shown here with error bars as SEM (n=3).

Figure 3 - Attenuated tumor formation in CCR1- and CCL3-deficient mice at 10 months after DEN treatment. Livers were obtained from mice at 10 months after DEN treatment to examine the presence of HCC foci. Among tumor-bearing mice of each strain (WT mice, n = 5; CCL3-deficient mice, n = 7; CCR1-deficient mice, n = 12), the relative ratios of liver to body weights (*a*), foci number per cm² (*b*), and the proportion of tissues occupied with tumor foci (*c*) were determined as described in Material and Methods. Each value represents mean \pm SEM. * indicate $p < 0.05$, compared with WT mice.

Figure 4 - Reduced IMVD and Kupffer cell numbers in liver of DEN-treated CCR1- and CCL3-deficient mice. (*a* and *b*) Livers were obtained from each strain at 10 months after DEN treatment and processed for immunostaining with anti-CD34 antibodies. IMVD was defined as the microvessel numbers per field at 200-fold magnification (*a*) or the proportions of CD34-positive areas (*b*) as described in Material and Methods, each value represents mean \pm SEM (n=5). * indicate $p < 0.05$, compared with WT mice.

(*c*) Livers were obtained from each strain at 10 months after DEN treatment and processed for immunostaining with an anti-F4/80 monoclonal antibody. The numbers of F4/80-positive cells in non-tumor and tumor areas were determined as described in Material and Methods. Each value represents mean \pm SEM (n=5). *, $p < 0.05$; **, $p < 0.01$.

Figure 5 - (*a* to *c*) Gene expression of angiogenic factors and their receptors, and matrix metalloproteinases. (*a*) RT-PCR for the genes of angiogenic factors and VEGF receptors was performed on total RNA extracted from WT mice liver at the indicated time intervals (0, 2, 4, 6 and 10 months) after DEN treatment, as described in Material and Methods. The ratios of each gene to β -actin were determined. Each value represents mean \pm SEM (n=5). m, month.

(b) RT-PCR for MMP and TIMP genes was performed on total RNA extracted from WT mice liver at 0, 2, 4, 6, and 10 months after DEN treatment, as described in Material and Methods. The ratios of each gene to β -actin were determined. Each value represents mean \pm SEM (n=5) with ** indicating $p<0.01$, compared with 0 month. m, month.

(c) RT-PCR for the indicated genes was performed on total RNA extracted from tumor bearing liver of WT, CCR1-, and CCL3-deficient mice at 10 months after DEN treatment in a separate experiment from the experiments shown in Figure 5a and b, as described in Material and Methods. The ratios of each gene to β -actin were determined. Each value represents mean \pm SEM (n=5) with ** indicating $p<0.01$, compared with WT mice.

(d) Immunohistochemical detection of MMP9-positive cells in liver after DEN treatment. Immunohistochemical analysis was performed on liver tissues obtained from WT, CCL3- or CCR1-deficient mice at the indicated time intervals after DEN treatment, as described in Material and Methods. Representative results from 6 individual animals are shown here. Original magnification, $\times 400$. Scale bars, 50 μ m.

(e) The numbers of MMP9-positive cells in WT, CCL3- or CCR1-deficient mice liver at 10 months after DEN treatment. All values and bars represent the mean and SEM calculated on the results from 6 individual animals, respectively. **, $p<0.01$.

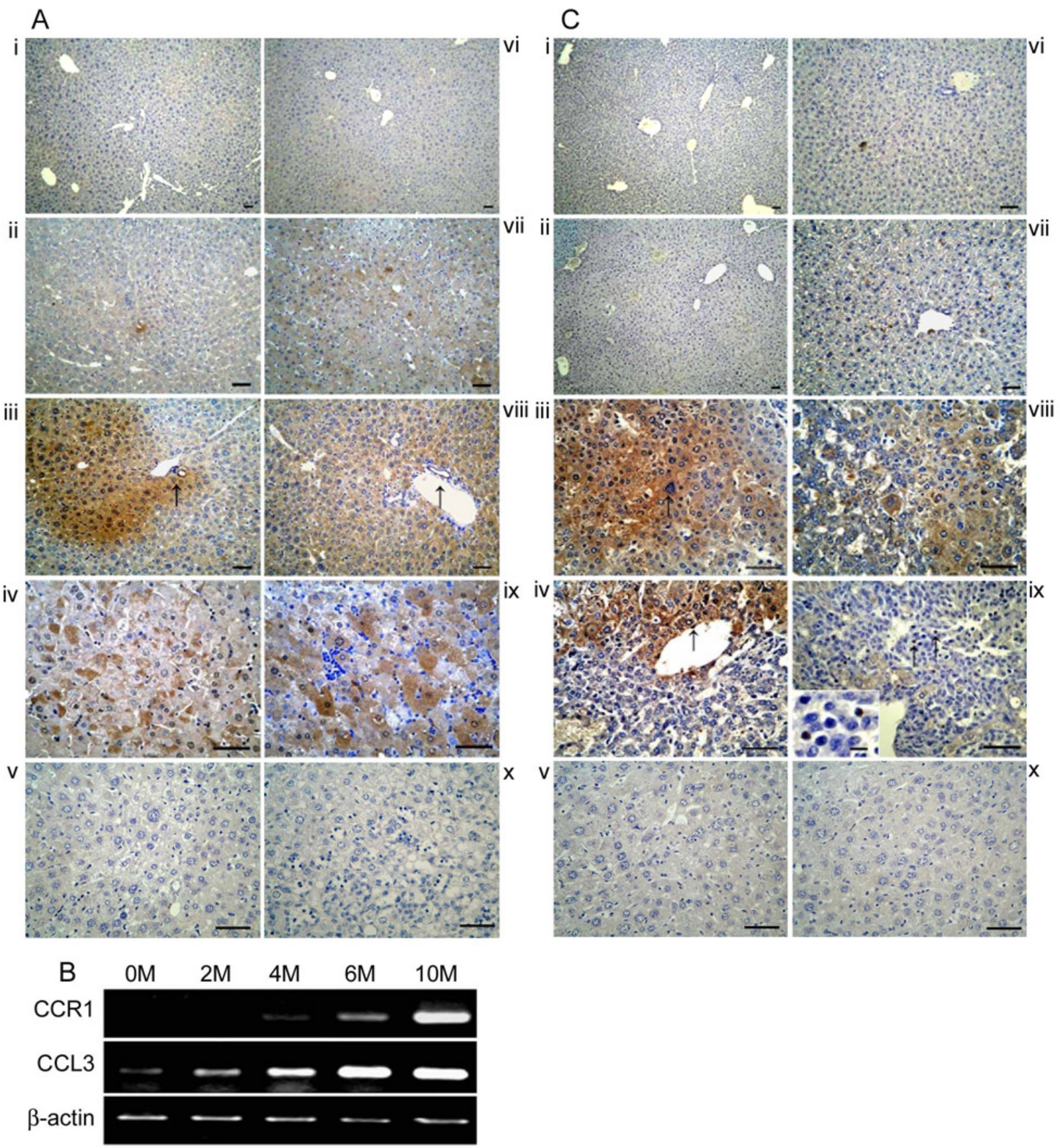
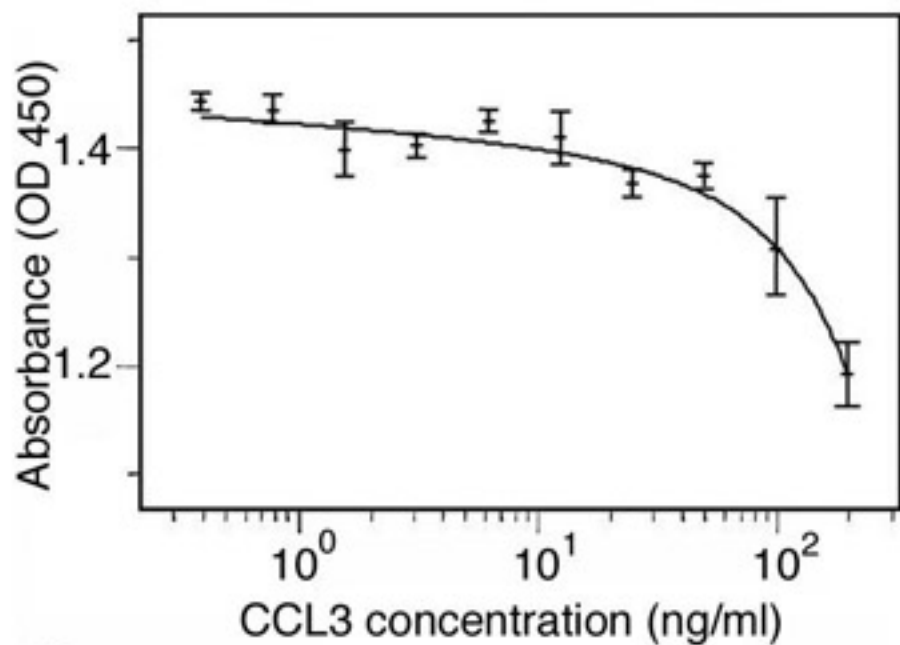


Fig 1

Yang et al. (Fig. 2)

A



B

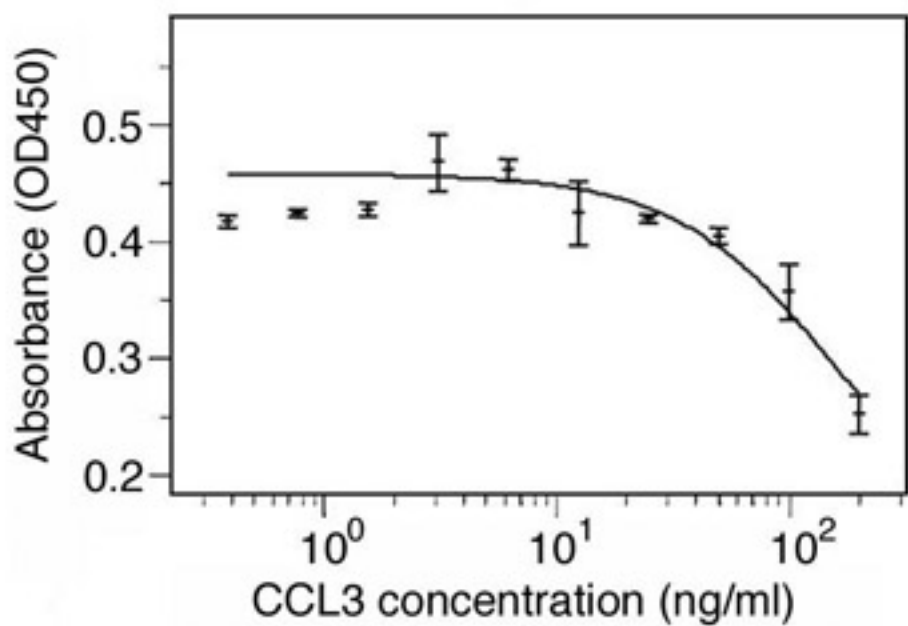


Fig 2

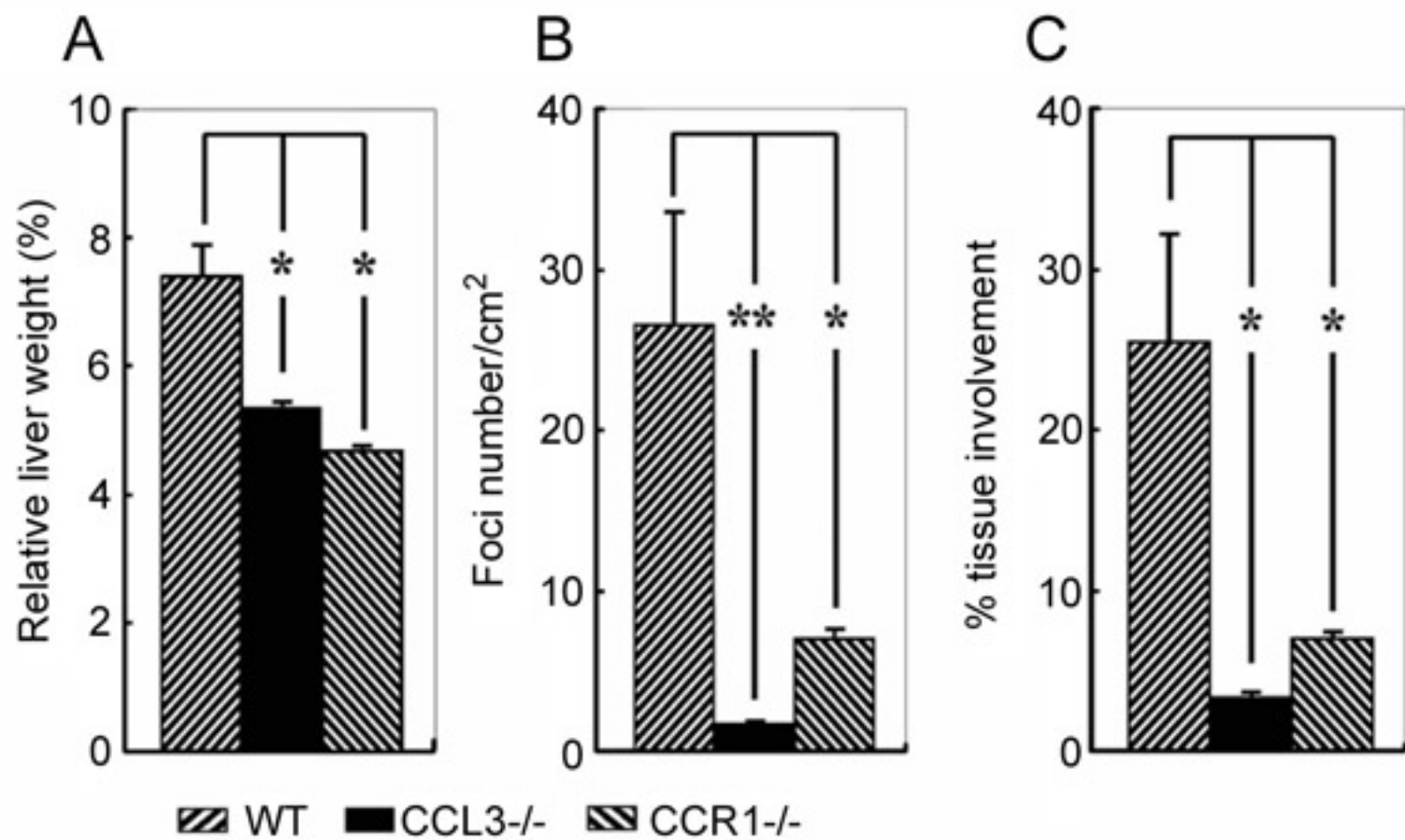


Fig 3

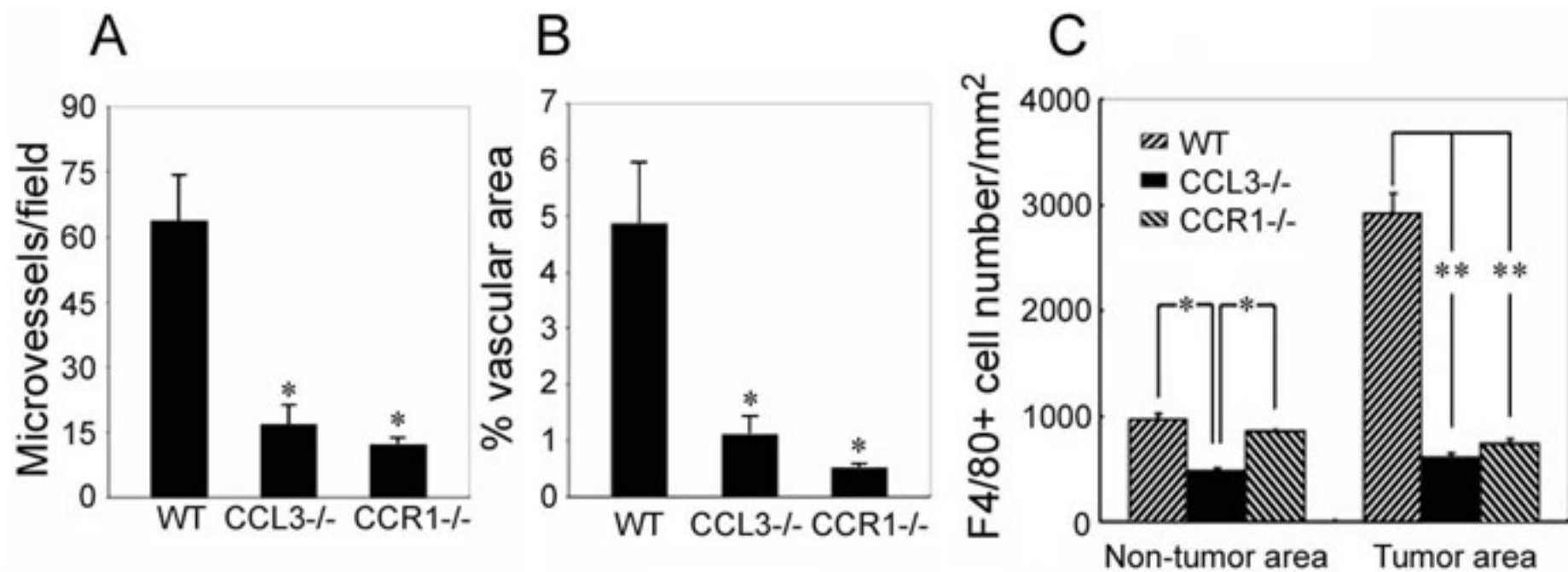


Fig 4

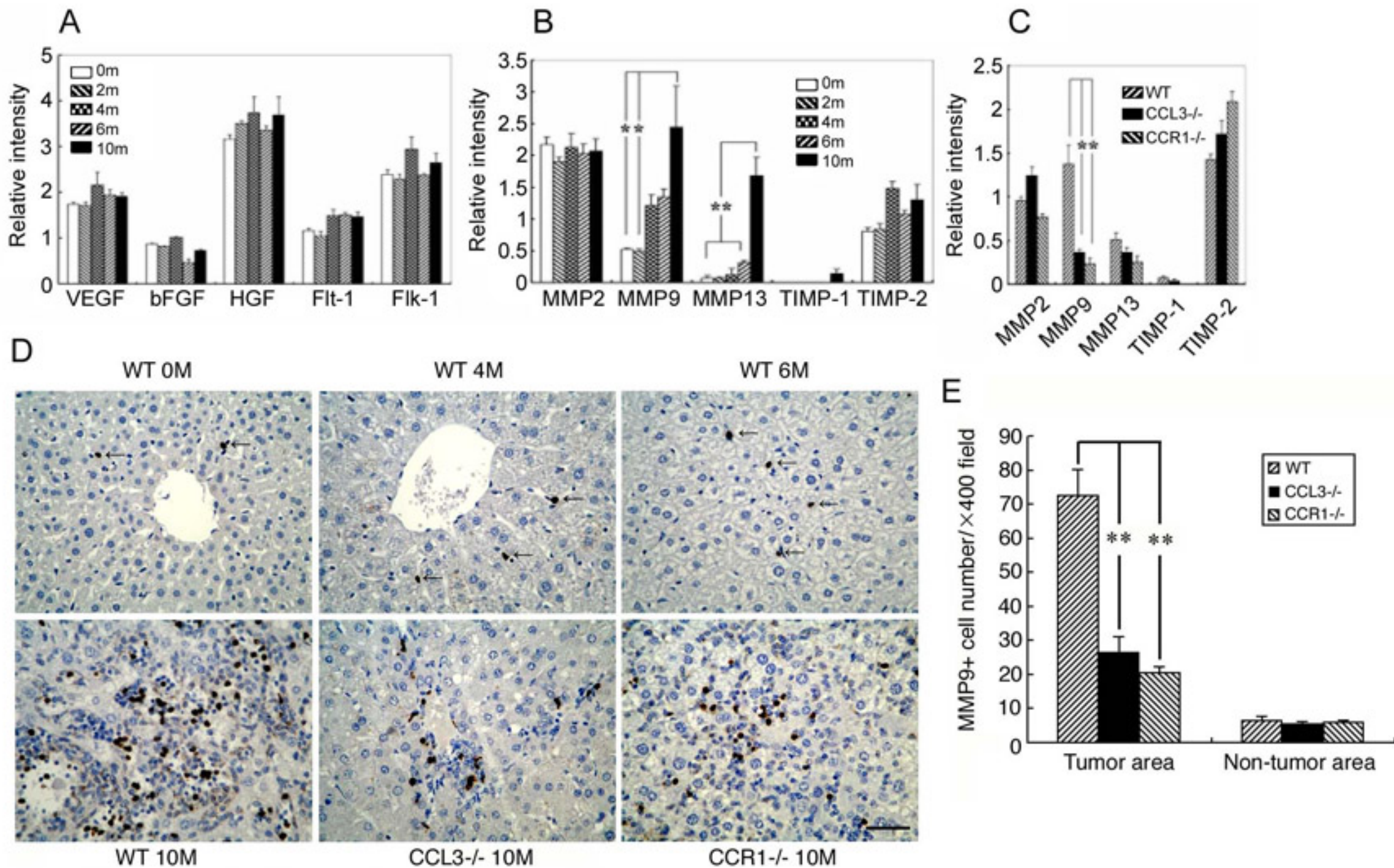


Fig 5